Study of high strength wheat flours considering their physicochemical and rheological characterisation as well as fermentation capacity using SW-NIR imaging.

Samuel Verdú[1*], Eugenio Ivorra[2], Antonio J. Sánchez[2], José M. Barat[1], Raúl Grau[1]

[1]Departamento de Tecnología de Alimentos. Universidad Politècnica de València, Spain.

[2] Departamento de Ingeniería de Sistemas y Automática, Universidad Politècnica de València, Spain

*Author for correspondence: Samuel Verdú

Address: Edificio 8G - Acceso F – Planta 0

Ciudad Politécnica de la Innovación

Universidad Politécnica de Valencia

Camino de Vera, s/n

46022 VALENCIA – SPAIN

E-mail: saveram@upvnet.upv.es

Phone: +34 646264839

Abstract

Characterisation of wheat flour destined for the bread-making process using hyperspectral image analyses based on Short-wave NIR imaging (SW-NIR) was studied. The first step was to characterise wheat flour batches by considering physicochemical, rheological and fermentation kinetic parameters. The second step was to capture the hyperspectral images of each batch. The results showed some significant differences in fermentation capacity in relation to gluten and its protein sub fractions. However, no significant rheological differences were observed. The acquired images were firstly analysed by a principal component analysis, where a clustering tendency was observed. Then linear correlations map was done to study the relationship between the SW-NIR spectra response and the physicochemical, rheological and fermentation kinetic parameters. The results showed an important correlation between the SW-NIR spectra (760-900 nm) and the fermentation capacity parameters of the batches, as well as gluten and its sub fraction proteins. The SW-NIR imaging analysis enabled to obtain useful information about wheat flour behavior related to the fermentation process. Thus the studied technique may represent a useful, rapid non-destructive method to help characterise wheat flours with non-different rheological parameters by considering their behavior during the fermentation process.

Keywords: SW-NIR image analysis, wheat flour, characterisation, fermentation

1. Introduction

Producing wheat and its by-products is a large sector in the food industry. Both kernels and their transformation have become a fundamental part of world economics. Cereals also represent the principal energy and nutrient source in the food chain (Fava et al., 2013). Thus the continuous improvement of processes and production methods is important to obtain better yields of raw materials and products. Although the processes used during transformations are well-known, there are some factors that still have room for improvement. These factors greatly influence processing and lead to repercussions in final products. Variations in the raw material could represent a problem during transformation and the production of final products with non-conformities given the corresponding loss of quality. Climatologic conditions during plant growth, the methods used to store kernels and the milling process all influence the characteristics of the resulting flour. Different cultivars are also an important factor for flour behavior. Therefore, identifying the best mixtures of wheat varieties is fundamental to guarantee best flour performance during production processes (Uthayakumaran et al., 1999). It is necessary, therefore, to thoroughly analyse each batch to ensure accurate characterisation and classification by producers, who can thus offer a homogeneous product with optimal technological characteristics. Likewise, the transformation industry requires accurate classification to adapt its processes by considering both the product formula and process variables. For this reason, monitoring raw material is an important phase in the production processes of cereals and flour. For wheat flour in particular, there are standard characterisation methods based on chemical composition (moisture, protein, dry gluten, ash, etc.) and rheological properties (Chopin alveograph, Brabender farinograph, RVA (Rapid Visco Analyser), etc). In short, a large amount of data is used to classify wheat flours. Although the relationships between the factors during processing are well-known, there are many which are quite difficult to control, especially when they interact. These unexpected factors could result from alterations in processing and non-conformities in the final product, such as loaf dimensions, crumb texture, visual crust aspect and bread consistency (Li Vigni et al., 2010).

It is, therefore, crucial to conduct new studies to make advances that improve the end product which are as constant as possible to satisfy consumer needs (Li Vigni et al., 2010). Traditional methods involve sound economic investment in either laboratory equipment or external analyses, and also in qualified personnel and numerous hours of labour. Therefore, the development of quick analysis methods that facilitate accurate wheat flour characterisation would be useful to help improve production efficiency. In this field, several authors have conducted research on new fast, non-destructive methods for monitoring both wheat kernel production and processed wheat flour (Arazur et al., 2012), which has been carried out using many different technologies. One of the most important areas of applied technology is the infrared spectra (IR) analysis, which employs a whole range of wavelengths. For example, Shao et al., (2011) predicted protein and starch levels in flour by studying the IR response with a spectrophotometer. Similarly, methods to characterise flours that consider their properties during the bread-making process (Li Vigni et al., 2009), classification of different categories of flour batches (Cochi et al., 2005) and predictions of the milling and baking parameters of different wheat varieties have been developed (Jirsa, et al., 2008). Characterisations through NIR technology of some bread-making process phases, such as the leavening phase, have also been reported. Specifically, Li Vigni & Cocchi (2013) described that there were differences among mixtures based on NIR spectrum variability if compared to leavening time. Fewer studies into the short-near infrared image analysis of raw materials have been conducted. Manley et al., (2011) characterised water diffusion through wheat kernel tissues. Xing et al., (2011) compared the results of infrared spectrophotometry and hyperspectral image analyses to study alpha-amylase activity determination. Singh et al., (2009) used the same method to detect insect damage to wheat kernels. Research into the relationship between hyperspectral image analyses and toxic metabolites of wheat fungus has also been conducted (Del Fiore et al., 2010). The present work aimed to study the capability of an SW-NIR camera to detect differences between wheat flours which did not show differences in routine industrial analyses, but indicated different fermentation behavior.

2. Material and methods

2.1 *Assay development*

The study was performed on six different wheat flour batches sold as “high-strength flour” employed for bakery products, sliced bread and sponge cakes (Molí del Picó-Harinas Segura S.L, Valencia-Spain). Batches were obtained during six consecutive weeks (B1, B2, B3, B4, B5 and B6). Firstly wheat flour batches were characterised according to their physicochemical and rheological features, SW-NIR image captures and their kinetic fermentation parameters by the structured light (SL) vision technique. Then according to the statistical results obtained from the SW-NIR image captured, the data of batches B2 and B5 were regrouped and recoded as GA and, in the same way B4 and B6 were regrouped and recoded as GB. A new flour sample (50% mix) was also generated by mixing 25% of flours B2, B5, B4 and B6. For this new flour sample, more analyses were carried out using the SW-NIR and SL techniques, and the statistical analysis was redone, but the new samples codification was taken into account. Finally, according to the information obtained from these two previous steps, a statistical correlation between the physicochemical and rheological characteristics and the kinetic fermentation parameters with the information acquired from the spectra of the captured SW-NIR image, was carried out.

2.2. Dough preparation and fermentation process

The ingredients employed and percentages used were: 56% wheat flour, 35% water, 2% refined sunflower oil (maximum acidity 0.2º Koipesol Semillas S., Spain), 2% commercial pressed yeast (Saccharomyces cerevisiae, Lesafre Ibérica S.A, Spain), 4% white sugar (≥ 99.8% sucrose. Azucarera Ebro, S.L, Spain) and 1.5% NaCl (refined marine salt ≥ 97% NaCl. Salinera Española, S.A, Spain). Dough was made by mixing all the ingredients in a food mixer (Thermomix® TM31, Vorwerk, Germany) according

to the following method. In the first phase, the liquid components (water and oil), sugar and NaCl were mixed for 4 min at 37°C. Pressed yeast was added in the next phase and was mixed at the same temperature for 30 sec. Finally, flour was added and mixed with the other ingredients using a default bread dough-mixing programme, which provides homogeneous dough. This programme was based on mixing the ingredients with the mixer helix turning randomly in both directions (550 revolutions/minute). This process was applied for 4.5 min at 37ºC. Next 450 g of dough (approximately 1-cm thick) were placed into a metal mould (8x8x30 cm) for fermentation. This was carried out in a chamber with controlled humidity and temperature (KBF720, Binder, Tuttlingen, Germany) where a 3D Structured Light (SL) device was developed and calibrated. The fermentation process conditions were 37°C and 90% Relative Humidity (RH). Samples were fermented until dough stability and size were lost (Ft) when growth depletion occurred, which was assumed when 3D imaging started to report dough area values by describing asymptotic behavior and a decrease of area values.

2.3 Characterisation of batches

2.3.1 Physicochemical analysis

The multiple physicochemical and rheological parameters were analysed for all the wheat flour batches to characterise them. Each analysis was performed in triplicatefollowing the standard methods of the International Association for Cereal Science and Technology (ICC), except for fractionation of gluten proteins, which was based on the method described by Graveland et al. (2000). The analysed parameters were the following: percentage of moisture (H), gluten (G), gliadin (GLI), glutenin (GLU), and alveograph parameters (P=maximum pressure (mm), L=extensibility (mm); W=strength (J^{-4})) (ICC standard No.121).

2.3.1 SW-NIR data acquisition and processing

The images of the 12 samples in each batch were taken by a Photonfocus CMOS camera MV1-D1312 40gb 12 (Photonfocus AG, Lachen, Switzerland) and a SpecimImSpector V10 1/2″ filter (Specim Spectral Imaging, LTD., Oulu, Finland), which works as a linear hyperspectral camera. The illuminant was an ASD illuminator reflectance lamp (ASD Inc, Boulder, USA), which produces stable illumination over the full working spectral range.

Samples were placed in a glass Petri dish (10-cm diameter) and spectra were collected directly at room temperature with no sample treatment.

The positions of the illuminant and camera in relation to the sample always remained constant in order to control the lighting conditions and to obtain a constant image size. The distance between the illuminant and the sample was 0.525 m, while that between the camera and the sample was 0.225 m. The obtained image (scanned line) was composed of 256 grey levels (8 bits). The diffuse reflectance spectrum was collected using 53 different wavelengths (each wavelength was digitalised with 8 bits). These wavelengths were distributed at intervals of 11.2 nm within the 400-1000 nm range. The scanned line was composed of 1,312 points, so images were recorded at a resolution of 1312 x 1082 pixels. The camera was operated by the developed software based on SDK Photonfocus-GigE_Tools using programming language C++.

Reflectance calibration was performed to normalise non-linear light source reflectance. This was done by applying Equation 1, where *rW* is the reflectance value of a white pattern reflectance acquired under the same conditions, *rD* is the dark measure covering the camera objective and *rS* is the sample reflectance.

$$R(\lambda) = \frac{(rS - rD)}{(rW - rD)} \qquad (2)$$

The other operations carried out on the spectra for further statistical processing were Standard Normal Variety. Image reflectance calibration and preprocessing were performed using a code developed with Matlab R2012a (The Mathworks, Natick, Massachussets, USA).

2.3.2 Monitoring fermentation by the ¨Structured Light¨ method (SL) and image processing.

The purpose of the 3D vision system was to obtain the 3D profile of the samples during fermentation. In order to accomplish this objective, the 3D vision system specifically developed in a previous study was used to monitor fermentation (Ivorra et al., 2013). This vision system was composed of a network graycamera (In-Sight 5100, Cognex, Boston, Massachusetts (USA)) and a red linear laser (Lasiris SNF 410, Coherent Inc. Santa Clara, California (USA)), both of which were placed inside the fermentation chamber.

The 3D visual system had a resolution of 2.1*10-4m and 1.4*10-4 m for axes X and Z, respectively. This resolution came from laser angle β of 0.65 radians in combination with the camera resolution (640x480) and its distance from the sample. The working range was 0.1 m on the X axis and 0.08m on the Z axis.

The acquisition rate was 1 fps due to the long time required for fermentation (around 2 h). The equipment was calibrated by calculating a homography transformation (Zhang, 2000) by taking 10 regularly distributed points on the laser projection plane with known coordinates (Trobina et al., 1995), and then using these 3D points and their corresponding points on the image.

The 3D sample profile was a 3D curve composed of the 3D points that lay between the known points of the mould's borders. In order to obtain these points, the first step was

the segmentation of the laser points on the image captured by the camera using an Otsu's global threshold (Otsu, 1979). Then these pixels were filtered by removing non-connected pixels with an area under 100px. Subpixel precision was achieved by calculating the exact row coordinate by the weight mean for each column using the intensity value.

The next step was the transformation from image coordinates to a 3D local coordinate system using the homography transformation calculated previously in the calibration step. The final step was to transform the local coordinate system by a rotation matrix which makes the z axis normal to the surface. The transversal area (A) (the integration of the Z values along the X direction of the sample) was extracted continuously from the 3D sample profile to analyse sample growth during fermentation with time, together with the maximum transversal area time (Ft).

Acquisition and data processing were carried out using a code developed in the Matlab 2012b computational environment (The Mathworks, Natick, Massachussets, USA).

2.3.2.1 Fitting the dataset to the Gompertz prediction model.

To model behavior during fermentation, the data set of the SL method, obtained from the six replicated doughs per wheat flour batch, was fitted to the Gompertz prediction model. The Gompertz function is a non-linear sigmoid growth function that was developed by Gompertz (1825) to calculate the mortality rates of microorganisms. The equation is as follows:

$$t = A \exp\ (-\exp\left(\frac{V}{A}(Lt - t) + 1\right)) \qquad (1)$$

where *t* is time, *A* is the maximum area of the process, *V* is the maximum growth rate, and *Lt* represents the latency time . The model parameters were determined using a non-linear regression procedure and were obtained by minimising the sum of the squares of the prediction errors.

2.4 Statistical analysis

The physicochemical, rheological and fermentation parameters (H, G, Gli,Glu, Gli/glu, P, L, P/L, W and A, V, Lt and Ft) were studied by a one-way variance study (ANOVA). In the cases where the effect was significant (P-value < 0.05), the means were compared by Fisher's least significant difference (LSD) procedure. The relationship between the data from the physicochemical and rheological analysis, as well as the fermentation kinetics, was carried out by linear correlation. The SW-NIR data spectra were analysed by the multivariate statistical procedure for which a principal component analysis (PCA) was used. The procedures were performed with PLS Toolbox 6.3 (Eigenvector Research Inc., Wenatchee, Washington, USA), a toolbox extension in the Matlab 7.6 computational environment (The Mathworks, Natick, Massachusetts, USA).

2. Results and discussion

3.1 Characterisation of batches

3.1.1 Physico-chemical analysis and fermentation kinetics

The six different distinct wheat flour batches were analysed for all the parameters. Table 1 shows the results of the battery of analyses, which indicate that no differences were found in the H, Lt and alveograph parameters. However, significant differences in the amount of gluten, gliadin, glutenin, and also in A, V and Ft, were observed. The

differences in gluten and its protein fractions can help understand the behavior observed during the fermentation process, where differences between the dough development kinetic parameters were seen (Ivorra et al., 2013). Figure 1 shows the average of the evolution of the A values for the six flour type replicates processed (B1, B2, B3, B4, B5 and B6). It is important to observe the differences between them. B2 and B5 presented the highest non-different A values, followed by B3. Finally B4, B6 and B1 gave the lowest values. *Ft* followed the same behavior as A. No significant differences were found for V and Lt.

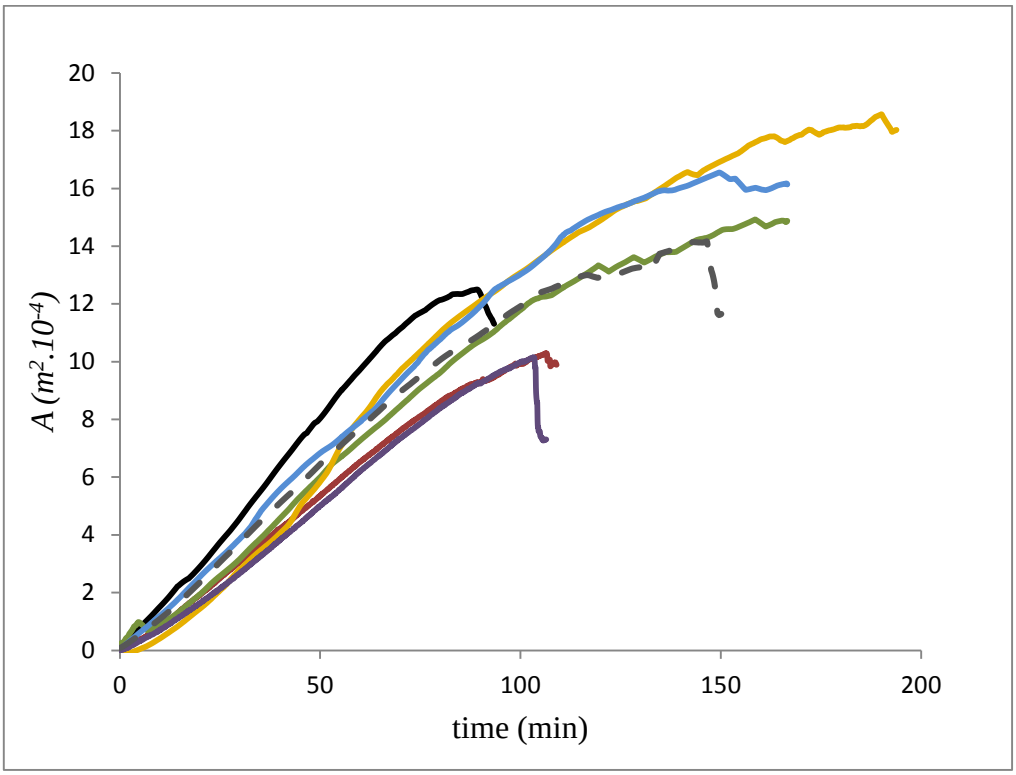

Figure 1. Evolution of the transversal area of the dough (A) with fermentation time (until growth depletion occurred). Dough series are represented by the following colours: B1 —; B2 —;B3 —; B4—;B5 —;B6—; and 50% mix of GA (50% B2 + 50% B5)/GB (50% B4+ 50% B6) ––.

To obtain preliminary overall knowledge about the relationship between wheat flour composition and fermentation capacity (maximum dough growth), correlation maps of both data groups were performed (Table 2).

When analysing the results of the correlations, only A and Ft presented a high R^2 of correlation with several physicochemical parameters. A related closely to G (R^2 = -0.825), Glu (R^2 = -0.860) and Gli/Glu (R^2 = 0.859). A good correlation with P (R^2 = 0.882) and Gli (R^2 = 0.866) was also found. Likewise, Ft presented correlated strongly to G (R^2 = -0.907), Glu (R^2 = -0.922) and Gli/Glu (R^2 = 0.928). In this case, Ft also correlated well with P (R^2 = 0.891), but correlated less with Gli (R^2 = 0.756). Evidently, gluten and its protein sub fractions affected fermentation behavior (Barak et al., 2013). The amounts of G, Glu and Gli were the main differences found between batches, so they could be the principal factors that influence fermentation parameters such as resistance to gas pressure and dough stability, which depend largely on these characteristics (Park et al., 2006). The fermentations of B2 and B5 showed significant differences if compared to B1, B4 and B6, whose fermentations were approx. 40% lower than A. B6, B1 and B4 also presented different characteristics for values A and Ft. Specifically, B1 and B6 reached a similar A value, but B4 was significantly higher, while Ft was quite low in these the batches if compared to the other batches showing high development. B2 and B5 also presented the lowest amount of Glu and, therefore, a higher Gli/Glu ratio. Previous research works by several authors have postulated that the amount of gliadin and glutenin, and an optimum ratio between them (Gli/Glu), are the main factors that affect fermentation characteristics (Veraverbeke & Delcour., 2002). These factors may result in different capacities to retain gas and provide different A and Ft values. It is likely that B1 and B4 (which presented the lowest *A* and *Ff* and the largest amount of glutenin, but not gliadin) had an unbalanced ratio as they had too

much glutenin, which meant increased dough tenacity. This may have been an impediment to reach high A and Ft values.

3.1.2 SW-NIR imaging analysis

The mean SW-NIR spectra for each wheat flour batch are represented in Figure 2-A, which shows different activity zones for the spectra. Both the visible and infrared zones presented peaks, which could offer information about samples. Thus in order to analyse this information and to evaluate whether the spectra reported useful data about samples, all the spectra were processed. A PCA was carried out after the Standard Normal Variety (SNV) pretreatment.

Figure 3-A shows the PCA space obtained for the first and second PCs (which explained 86.64% of variance) of the complete spectra. Only the first two PCs were taken into account as they were considered to sufficiently explain variance. A tendency of groups across PC2 is observed. This tendency shows how flour batches were positioned in different PC2 zones and how a fermentation behavior relationship was maintained (Fig. 3). We can see how B2 and B5 are positioned in the positive values zone of PC2, and how B4 and B6 are isolated in the negative values zone of PC2. However, B1 and B3 appear in the middle of both zones, but have no significant differences if compared to the other batches. Although B1 and B3 are not positioned in a specific zone like the other samples, we could see their tendency to cluster; B1 tends towards the zone where B4 and B6 are placed, while B3 tends towards the zone of B2 and B5.

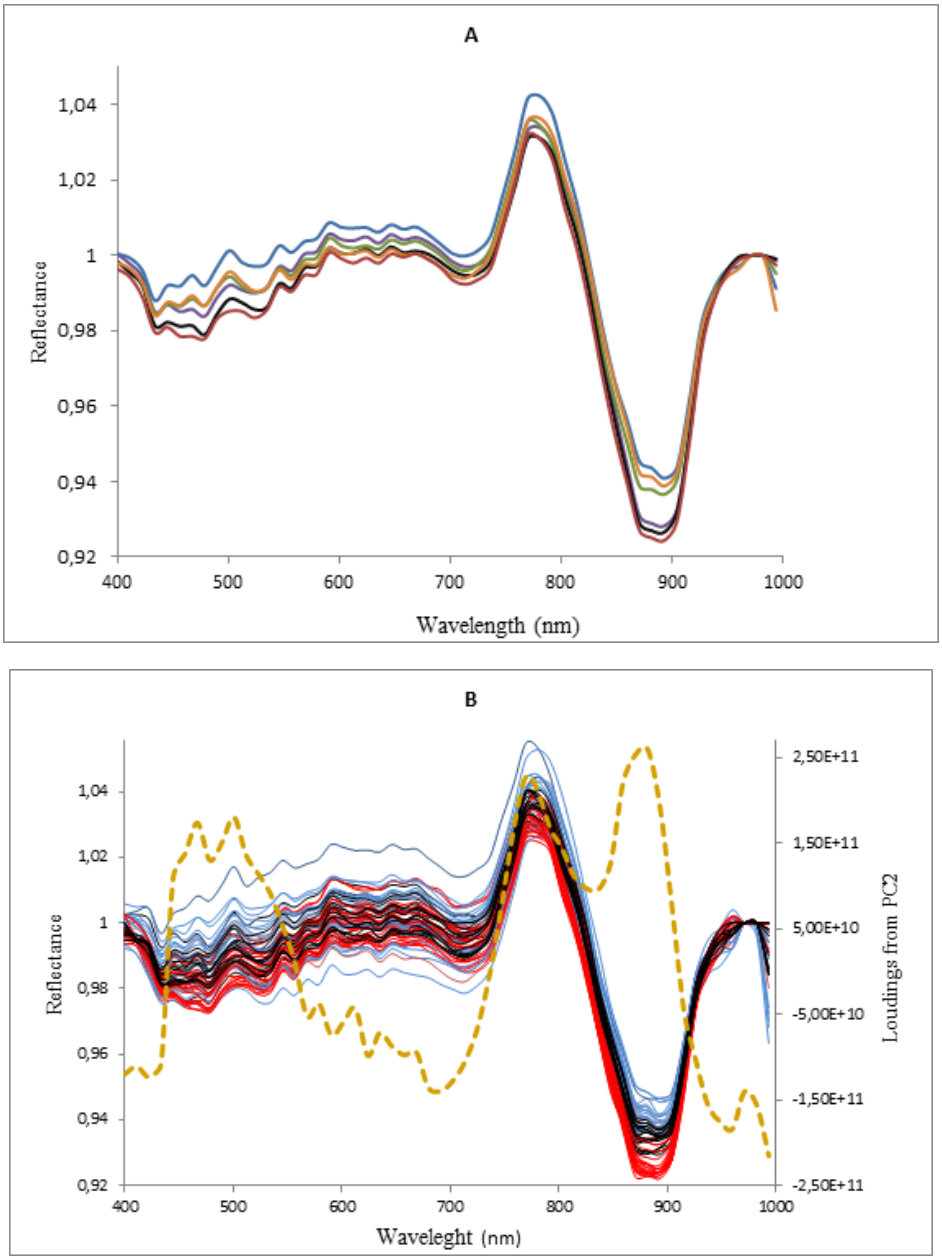

Figure 2.

A: Means of the spectra response for each wheat flour batch. B1 ; B2 ; B3 ; B4 ; B5 ; B6 .

B: Set of spectra responses of GA (B2+B5) , GB (B4+B6) and a 50% mix . Loadings from the PC2 ---.

Following these results, extremely placed batches with no differences between them were studied in conjunction as a single sample. This meant that data sets B2 and B5 were recorded as a single sample called GA, and B4 and B6 as one named GB. Given the aim to prove the observed phenomena, a new flour sample was also created to be analysed by the imaging analysis like the initial flours. This new sample (50% mix) was the result of mixing 25% of B2 + 25% of B5 + 25% of B4 + 25% of B6. Another PCA was performed with the information acquired from the recoded GA and GB and the data from the new sample (50% mix). Figure 3-B shows the obtained PCA space, where the same clustering tendency as in the previous study is seen (Fig. 5-A), and where samples were clustered mainly by PC2. GA (B2+B5) was placed in the positive PC2 zone, while GB (B4 + B6) was placed in its negative zone, with the 50% mix sample placed in the middle. To assess the information from PC2, the loadings were plotted across the studied wavelength (the dashed line in Figure 2-B). The peaks of the loadings were observed in both the visible and infrared spectra zones. However the PCA analysis, carried out by employing only the information from either the visible spectra or the SW-NIR spectra, gave a higher explained variance value for the latter (78% and 90.5% of total variance captured, respectively).

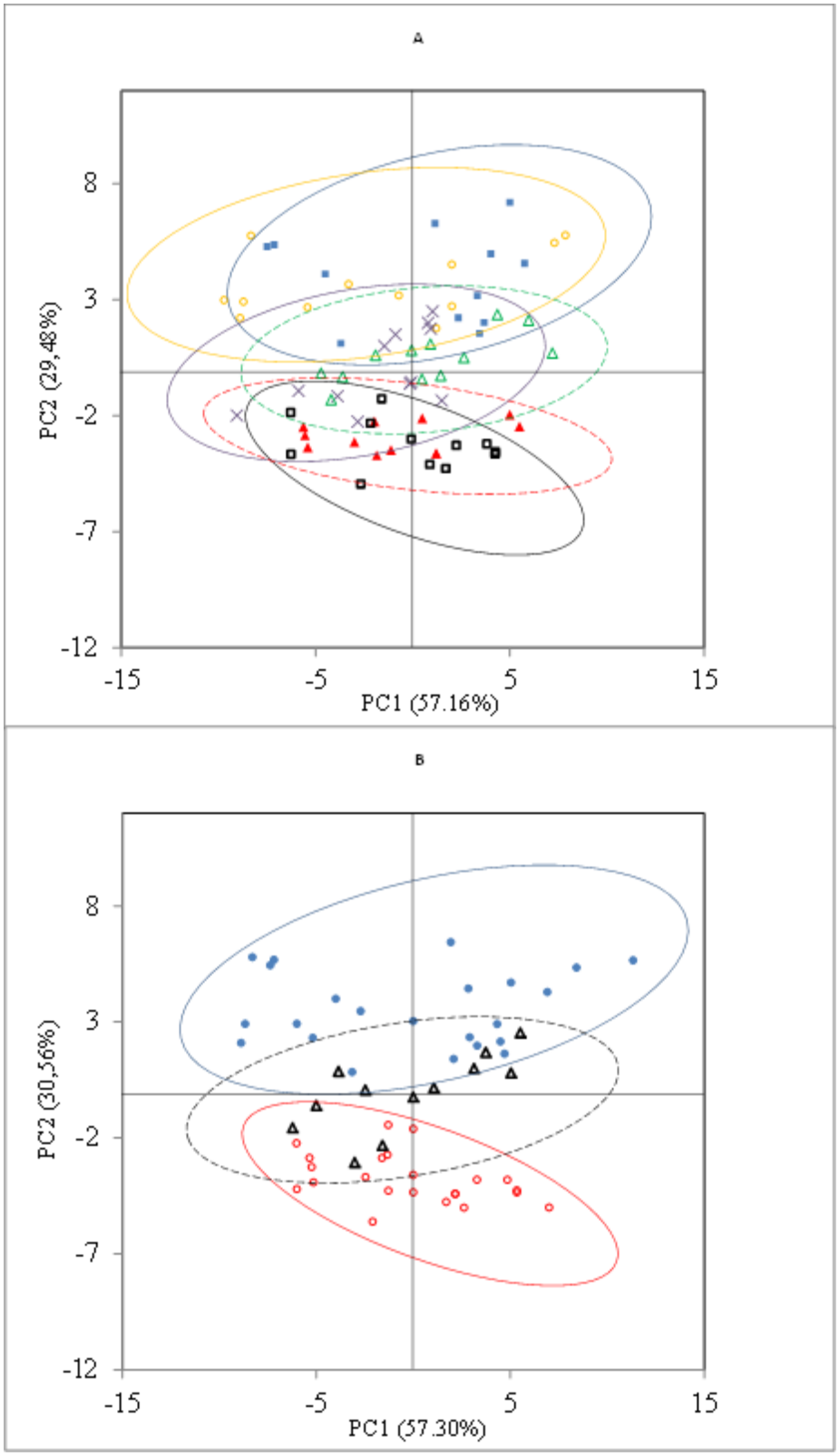

Figure 3. PCA Studies.

A: Scores plot of the first two PCs calculated by PCA based in the mean spectra from all the analyzed batches. B1x;B2■;B3Δ;B4□;B5○;B6▲.

B: Scores plot of the unique two PCs calculated by PCA based in the mean spectra of GA (●), GB (○) and 50% mix of them (Δ). Circumferences mark significant differences.

In order to compare the behavior of the 50% mix wheat flour during its fermentation with the performance noted for the wheat flours used to make up the mixture, a new fermentation study was conducted. The result of its growth curve is included in Figure 1 (discontinued black line). The fermentation parameters, obtained by fitting the curve to the Gompertz equation (Table 3), obtained intermediate values between wheat flours GA and GB. So according to the results expressed in Figure 3-A and B and the values in Table 1, there was a parallelism between the physicochemical, kinetics parameters of fermentation and the information acquired from the SW-NIR measurements. Therefore, when comparing the A and Ft values (Tables 1 and 3) with the PCA results (Fig. 4-A and B), we can see that lower A and Ft values clustered in a different zone when considering flour batches with higher values. Furthermore, the flour batches with intermediate values were also positioned between the two previous zones. In order to evaluate this parallelism, correlations were carried out between the mean score of each batch from PC2 and the remaining physicochemical and rheological parameters (Table 2). The highest R^2 values were obtained for the following parameters: G, Gli, Glu, Gli/Glu, A and Ft.

Table 1. Physicochemical, rheological and fermentation characterisation of flour batches.

	B1	*B2*	*B3*	*B4*	*B5*	*B6*
H (%)	14.3 ± 0.1a	14.2 ± 0.2a	14.5 ± 0.1a	14.6 ± 0.0a	14.2 ± 0.1a	14.6 ± 0.1a
G (%)	13.0 ± 0.1b	12.0 ± 0.1a	12.8 ± 0.2b	13.1 ± 0.2b	11.6 ± 0.2a	13.05 ± 0.2b
Gli (%)	7.2 ± 0.1a	7.3 ± 0.2a	7.3 ± 0.3a	7.1 ± 0.2a	7.3 ± 0.4a	7.2 ± 0.2a
Glu (%)	5.8 ± 0.4b	4.7 ± 0.1a	5.5 ± 0.2b	5.9 ± 0.2b	4.4 ± 0.1a	5.9 ± 0.3b
Gli/Glu	1.2 ± 0.1a	1.5 ± 0.1b	1.3 ± 0.1a	1.2 ± 0.0a	1.7 ± 0.1b	1.2 ± 0.1a
P	96.5 ± 2.1a	97.0 ± 1.6a	97.5 ± 1.7a	96.0 ± 1.4a	98.0 ± 1.8a	96.0 ± 1.9a
L	105.0 ± 1.4a	108.0 ± 1.0a	106.5 ± 1.2a	106.5 ± 0.7a	107.0 ± 1.2a	105.5 ± 1.3a
W	374 ± 5.7a	382 ± 5.4a	387 ± 5.2a	375 ± 5.7a	375 ± 5.5a	374 ± 4.3a
P/L	0.92 ± 0.1a	0.90 ± 0.2a	0.92 ± 0.1a	0.91 ± 0.2a	0.92 ± 0a	0.91 ± 0.2a
A ($m^2.10^{-4}$)	10.6 ± 0.7a	18.0 ± 1.0dc	16.4 ± 0.8c	12.2 ± 0.7a	18.2 ± 0.5d	10.2 ± 1.0a
V ($m^2.10^{-4}$/min)	2.4 ± 0.2b	2.1 ± 0.4a	2.0 ± 0.1a	1.7 ± 0.0a	2.0 ± 0.1a	1.7 ± 0.2a
Lt (min)	1.7 ± 0a	1.6 ± 0a	2.0 ± 0a	1.8 ± 0a	2.0 ± 0a	2.1 ± 0.1a
Ft (min)	105.3 ± 3.5b	156.5 ± 4.0c	148.7 ± 5.0c	90.3 ± 1.4a	186.7 ± 5.0d	108,5 ± 4.8b

Values and standard deviation of composition parameters; H, moisture content; G, content of dry-gluten; Gli, gliadin content; Glu, glutenin content and Gli/Glu, ratio between gliadin and glutenin content. Alveograph parameters: P, maximum pressure; L, extensibility; W, strength. Fermentation parameters: A, maximum area; V, maximum growth rate; Lt, time of latency and Ft, final time. Values followed by different letters are significantly different at $P < 0.05$ between columns.

The results indicate that the link between the fermentation behavior and spectral response of the flour batches is probably, and mainly, the amount of gluten and its subfraction proteins, although other factors, such as starch, could also affect the process. They also proved that the amount of these components influences A and Ft directly and that they also related significantly to the SW-NIR spectra response. Thus although the entire spectrum was analysed, the main information, which could differentiate batches, was obtained at the interval from 760-900 nm approximately. The obtained results agree with the results reported in several previous studies, where relationships between both gluten and its sub fraction proteins to these spectra absorption bands have been found.

Table 2. Coefficients of correlation (R^2) between rheological, chemical and kinetic parameters of the doughs, included scores of principal component 2 (PC2), obtained by SL technique, and physicochemical and rheological parameters of the flour batches.

	G	Gli	Glu	Gli / Glu	H	A	Ft	L	Lt	P	P / L	W	Score PC2
G	1												
Gli	-0.646	1											
Glu	0.995*	-0.711	1										
Gli / Glu	-0.995*	0.710	-0.998*	1									
H	0.814	-0.622	0.823	-0.815	1								
A	-0.825*	0.866*	-0.860*	0.859*	-0.842	1							
Ft	-0.907*	0.756	-0.922*	0.928*	-0.571	0.799	1						
L	-0.724	0.458	-0.727	0.714	-0.443	0.664	0.761	1					
Lt	0.093	0.013	0.093	-0.068	0.482	-0.329	0.166	-0.301	1				
P	-0.794	0.904*	-0.830*	0.845*	-0.645	0.882*	0.891*	0.496	0.145	1			
P / L	0.083	0.263	0.063	-0.025	0.231	0.100	0.027	-0.534	0.456	0.400	1		
W	-0.145	0.701	-0.222	0.210	-0.058	0.504	0.421	0.498	-0.062	0.467	-0.075	1	
Score PC2	-0.937*	0.791	-0.958*	0.948*	-0.787	0.885*	0.836*	0.671	-0.209	0.794	-0.111	0.317	1

*Correlation is significant at 0.05 level.

By way of example, when evaluating the NIR spectra of the mixes with different gluten powder and starch proportions, Chen et al. (2006) observed that the absorbance of samples from 850 to 900 nm increased together with the gluten concentration in the mixed formulation. Sinelli et al. (2011) reported the possibility of predicting the amount of gluten in semolina for dried pasta by analysing the spectra from 830 to 2700 nm to thus discern the technological quality of raw material. The relationship between those absorption bands and functional groups has been reported by Murray (2004), who postulated that one of the maximum absorption peaks of groups R-NH_2 and R-NH-R, among others, fell within the 770-850 nm range. Therefore, the obtained spectra response within this wavelength range can be specifically associated with amine groups

and peptide bonds of proteins and gluten. In line with this, the observed correlations between the PC2 scores and the measured variables (Table 2) for each wheat flour batch could be explained by the differences between gluten and its sub fraction proteins.

Table 3. Fermentation characterisation of GA (B2+B5), GB (B4+B6) and a 50% mix (GA+GB) of flour batches.

	GA	*GB*	*50% mix*
A ($m^2.10^{-4}$)	18.1 ± 0.1a	11.2 ± 1.4c	14.1 ± 0.5b
V ($m^2.10\text{-}^4$/min)	2.1 ± 0.1a	1.7 ± 0a	2 ± 0.2a
Lt (min)	1.8 ± 0.3a	2.0 ± 0.2a	1.5 ± 0.3a
Ft (min)	171.6 ± 21.3a	107.6 ± 1.3b	143.4 ± 3.6ab

Fermentation parameters: A, maximum area; V, maximum growth rate; Lt, time of latency and Ft, final time. Values followed by different letters are significantly different at $P < 0.05$ between columns.

3. Conclusions

In this work, a relationship between the SW-NIR spectra obtained by the imaging analysis of non-different wheat flours was observed after considering the official quality analysis and their behavior during the fermentation process. Characteristics such as amount of gluten and its sub fraction proteins influenced the spectral response, which could be differentiated by multivariate analyses (PCA). These variations related directly to the fermentation behavior parameters obtained by the SL technique. Accordingly, the SW-NIR imaging analysis may be the basis of a useful online tool to quickly obtain information about the behavior of wheat flours during fermentation, while a rheological analysis shows no differences in their characterisation. More research should be carried out to obtain robust prediction models in order to develop industrial online bread-making imaging applications.

4. References

Arazuri, S. Arana, J. I., Arias, N., Arregui, L. M., Gonzalez-Torralba, J., Jaren, C. 2012. Rheological parameters determination using Near Infrared technology in whole wheat grain. Journal of Food Engineering 111 (1), pp. 115-121.

Barak, S., Mudgil, D. & Khatkar, B.S. 2013.Relationship of gliadin and glutenin proteins with dough rheology, flour pasting and bread making performance of wheat varieties. Food Science and Technology, 51, 211-217.

Chen, Z., Morris, J., Martin, E. 2006. .Extracting chemical information from spectral data with multiplicative light scattering effects by optical path-length estimation and correction. Analitical Chemistry, 78, 7674-7681

Cocchi, M., Corbellinib M., Focaa, G., Lucisanoc, M., Paganic, M. A., Lorenzo T. & Alessandro, U. 2005. Classification of bread wheat flours in different quality categories by a wavelet-based feature selection/classification algorithm on NIR spectra.AnalyticaChimica Acta, 544, 100–107.

Cocchi, M., Corbellini, M., Foca, G., Lucisano, M., Pagani, M.A., Tassi, L., Ulrici. A. 2005. Classification of bread wheat flours in different quality categories by a wavelet-based feature selection/classification algorithm on NIR spectra. Analytica Chimica Acta 544 100–107.

Del Fiore, A., Reverberi, M., Ricelli, A., Pinzari, F., Serranti, S., Fabbri, A.A., Bonifazi, G., Fanelli, C. 2010. Early detection of toxigenic fungi on maize by hyperspectral imaging analysis. International Journal of Food Microbiology, 144 64–71.

Fava, F., Zanaroli, G., Vannini, L., Guerzoni, E., Bordoni, A., Viaggi, D., Robertson, J., Waldron, K., Bald, C., Esturo, A., Talens, C., Tueros, I., Cebrián, M., Sebok, A., Kuti, T., Broeze, J., Macias, M and Brendle, H. 2013. New advances in the integrated management of food processing by-products in Europe: sustainable exploitation of fruit

and cereal processing by-products with the production of new food products (NAMASTE EU). New Biotechnology. Volume 30, Number 6, September.

Gompertz, B. 1825. On the nature of the function expressive of the law of human mortality, and a new mode of determining the value of live contingencies. Philosophical Transactions of the Royal Society, 182, 513–585.

Graveland, A., Henderson, M.H., Paques, M., Zandbelt, P.A. 2000.Composition and structure of gluten proteins. In: Schofield, J.D. (Ed.), Wheat Structure, Biochemistry and Functionality. Royal Society of Chemistry, Cambridge, MA, pp. 90–99.

ICC – International Association for Cereal Science and Technology (Vienna-Austria).

Ivorra, E., Girón, J., Sánchez A., Verdú, S., Barat, J.M., Grau, R. 2013. Detection of expired vacuum-packed smoked salmon based on PLS-DA method using hyperspectral images. Journal of Food Engineering 117 342–349.

Ivorra, E., Verdú, S, Sánchez A., Barat, J.M., Grau, R. 2014. Continuous monitoring of bread dough fermentation using a 3D vision Structured Light technique. Journal of Food Engineering 130 8–13.

Jirsa, O., Hrušková, M., Švec, I., 2008. Near-infrared prediction of milling and baking parameters of wheat varieties, Journal of Food Engineering, 87 (1), pp. 21-25

Li Vigni, M., Durante, C., Foca, G., Marchetti, A., Ulrici, A., Cocchi, M. 2009. Near Infrared Spectroscopy and multivariate analysis methods for monitoring flour performance in an industrial bread-making process. Analytica Chimica Acta. 642 69–76.

Li Vigni M., Durante, C., Foca, G., Ulrici, A., Møller Jespersen, B.P., Bro, R., Cocchi, M. 2010. Wheat flour formulation by mixture design and multivariate study of its technological properties. Journal of Chemometrics, Volume 24, Issue 7-8.

Manley, M., du Toit, G., Geladi, P. 2011. Near infrared spectroscopy and multivariate analysis to evaluate wheat flour doughs leavening and bread properties. Analytica Chimica Acta 686, 64–75.

Murray, I. 2004. Scattered information: philosophy and practice of near infrared spectroscopy. Proceedings of the 11th International Conference on Near Infraredspectroscopy.NIR Publications 2.

Otsu, N. 1979. A Threshold Selection Method from Gray-Level Histograms. IEEE Transactions on systems, man, and cybernetics, 9, 66-69.

Park, S. H., Bean, S. R., Chung, O. K., &Seib, P. A. 2006.Levels of protein and protein composition in hard winter wheat flours and the relationship to breadmaking. Cereal Chemistry, 83, 418-423.

Shao, Y., Cen, Y., Yong He, Y., Liu, F. 2011. Infrared spectroscopy and chemometrics for the starch and protein prediction in irradiated rice. Food Chemistry, 126 1856–1861.

Sinelli, N., Pagani, M.A., Lucisano, M., D'Egidio, M.G., Mariotti.M.2011. Prediction of semolina technological quality by FT-NIR spectroscopy. Journal of Cereal Science, 54 218-223.

Singh, C.B., Jayas, D.S., Paliwal, J., White N.D.G. 2009. Detection of insect-damaged wheat kernels using near-infrared hyperspectral imaging. Journal of Stored Products Research 45 151–158.

Uthayakumaran S., Gras P.W., Stoddard F.L., Bekes F. 1999. Effect of varying protein content and glutenin-to-gliadin ratio on the functional properties of wheat dough. Cereal Chemistry, 76(3): 389–394.

Veraverbeke, W. S., &Delcour, J. A. 2002. Wheat protein composition and properties of wheat glutenin in relation to breadmaking functionality. Critical Reviews in Food Science and Nutrition, 42, 179-208.

Xing, J., Symons, S., Hatcher, D., Shahin, M. 2011. Comparison of short-wavelength infrared (SWIR) hyperspectral imaging system with an FT-NIR spectrophotometer for predicting alpha-amylase activities in individual Canadian Western Red Spring (CWRS) wheat kernels. Biosystems engineering, 108 303-310.

Zhang, Z. 2000. A flexible new technique for camera calibration. Pattern Analysis and Machine Intelligence, IEEE Transactions on, 22(11), 1330– 1334. doi:10.1109/34.888718

Alphabetical list of abbreviations

G: percentage of gluten

Gli/Glu: gliadin/glutenin ratio

Gli: percentage of gliadin

Glu: percentage of glutenin

H: percentage of moisture

A: area of dough reported by the 3D vision system

B: sample number code from a flour batch

Ft: time until the dough lost its stability and size

GA: SW-NIR data of batches B2 and B5

GB: SW-NIR data of batches B4 and B6

L: extensibility

Lt: latency time before the dough begins to develop

nm: nanometres

P/L: maximum pressure/extensibility ratio

P: maximum pressure

PC: principal component

PCA: principal component analysis

rD: the dark measure covering the camera's objective

RH: relative humidity

rS: sample reflectance

rW: the reflectance value of a white pattern

SL: Structured Light 3D vision technique

SNV: Standard Normal Variety pretreatment

SW-NIR: Short-wave Near Infrared

t: time

V: maximum growth rate

W: strength